(12)

DEVELOPMENT OF AN OPTICAL DISC RECORDER

QUARTERLY TECHNICAL REPORT

January 1 to March 31, 1977

Sponsored by

DEFENSE ADVANCED RESEARCH PROJECTS AGENCY

ARPA Order No. 3080
Program Code No. 6D30

Contract No. N00014-76-C-0441

Principal Investigator: George Kenney (914) 762-0300
Scientific Officer: Marvin Denicoff

Amount of Contract: $774,900
Contract Period: 1 Oct. 1975 - 31 May 1977

Prepared by

PHILIPS LABORATORIES
A Division of North American Philips Corporation
Briarcliff Manor, New York 10510

April 1977

UNCLASSIFIED

SECURITY CLASSIFICATION OF THIS PAGE (When Data Entered)

REPORT DOCUMENTATION PAGE		READ INSTRUCTIONS BEFORE COMPLETING FORM
1. REPORT NUMBER	2. GOVT ACCESSION NO.	3. RECIPIENT'S CATALOG NUMBER
4. TITLE (and Subtitle) DEVELOPMENT OF AN OPTICAL DISC RECORDER		5. TYPE OF REPORT & PERIOD COVERED Quarterly Technical Report 1 Jan. 1977 - 31 March 1977
		6. PERFORMING ORG. REPORT NUMBER
7. AUTHOR(s) G. Kenney, F. Zernike, D. Lou, M. Giebler, A. Milch, J. Wagner, A. Chan, R. McFarlane		8. CONTRACT OR GRANT NUMBER(s) N00014-76-C-0441
9. PERFORMING ORGANIZATION NAME AND ADDRESS PHILIPS LABORATORIES A Division of North American Philips Corp. Briarcliff Manor, New York 10510		10. PROGRAM ELEMENT, PROJECT, TASK AREA & WORK UNIT NUMBERS ARPA Order No. 3080 Program Code No. 6D30
11. CONTROLLING OFFICE NAME AND ADDRESS Defense Advanced Research Projects Agency 1400 Wilson Boulevard Arlington, Virginia 22209		12. REPORT DATE April 1977 13. NUMBER OF PAGES 43
14. MONITORING AGENCY NAME & ADDRESS (if different from Controlling Office) Office of Naval Research 800 North Quincy Street Arlington, Virginia 22217 Code: 437		15. SECURITY CLASS. (of this report) UNCLASSIFIED 15a. DECLASSIFICATION/DOWNGRADING SCHEDULE

16. DISTRIBUTION STATEMENT (of this Report)

Approved for public release: Distribution unlimited.

17. DISTRIBUTION STATEMENT (of the abstract entered in Block 20, if different from Report)

18. SUPPLEMENTARY NOTES

19. KEY WORDS (Continue on reverse side if necessary and identify by block number)

optical disc recorder
direct-read-after-write (DRAW)
lasers
substrate materials
recording materials
disc protective mechanism
disc
sled
air sandwich

20. ABSTRACT (Continue on reverse side if necessary and identify by block number)

Twenty tellurium air sandwiches were assembled in a new dedicated clean room. Preliminary tests of the sandwiches indicate acceptable characteristics for digital recording. The recorder prototype is now operational. The Philips Research Laboratories (PRL) recorder has been used for routine materials evaluation. No degradation of tellurium films has been observed after 3,000 hours at 90°C. The backup turntable and sled assembled from commercially available components were tested and found acceptable for digital recording applications. The tasks of data modulation and error encoding/decoding are proceeding well.

DD FORM 1 JAN 73 1473 EDITION OF 1 NOV 65 IS OBSOLETE

387334

UNCLASSIFIED

SECURITY CLASSIFICATION OF THIS PAGE (When Data Entered)

TABLE OF CONTENTS

QUARTERLY TECHNICAL REPORT
1 January 1977 to 31 March 1976

1. SUMMARY

Twenty tellurium air sandwiches were assembled in a new dedicated clean room. Preliminary tests of the sandwiches indicate acceptable characteristics for digital recording. The recorder prototype is now operational. The Philips Research Laboratories (PRL) recorder has been used for routine materials evaluation. No degradation of tellurium films has been observed after 3,000 hours at 90°C. A turntable and sled assembled from commercially available components were tested and found acceptable for digital recording applications. The tasks of data modulation and error encoding/decoding are proceeding well.

2. RESEARCH PROGRAM OBJECTIVES

The objective of this program is to develop an optical disc recorder of digital information, with a direct-read-after-write (DRAW) capability. A storage capacity of $>10^{10}$ bits is desired, with 4.4×10^5 bits on each of the 40,000 tracks of the disc. The desired error rate is 10^{-9} at a data rate greater than 1.33 Mbit/s. The key element in the proposed system is a recording material that can be exposed with a low-power laser (e.g., HeNe), leading to a recorder that could be manufactured for <$10,000 and discs that would cost <$10 in quantity.

3. SCHEDULE

The program schedule and milestones are given in Figure 1. First evaluation of the S-N ratios and defects (Task 1.3) for tellurium film recordings has been done. These preliminary

results indicate that tellurium is acceptable for recording digital signals.

The air sandwich disc design (Task 1.5) was finalized for the purposes of this program.

Life testing of tellurium and bismuth films continues. Both materials continue to exhibit acceptable properties for digital recording.

The assembly of a digital electronics subsystem (Task 2.2) was successfully completed with the checkout of the Miller modulator/demodulator and Linkabit encoder/decoder (Milestone 7b). This digital subsystem will be used in the first information storage and retrieval tests. A backup encoder/decoder is being constructed.

With incorporation of an improved focusing system in the prototype recorder, Task 2.3 was completed. The optical system incorporating a 25 mW HeNe laser is now operational. Milestone 8 and 10b were met, and system tests are planned for the next quarter (Task 2.6).

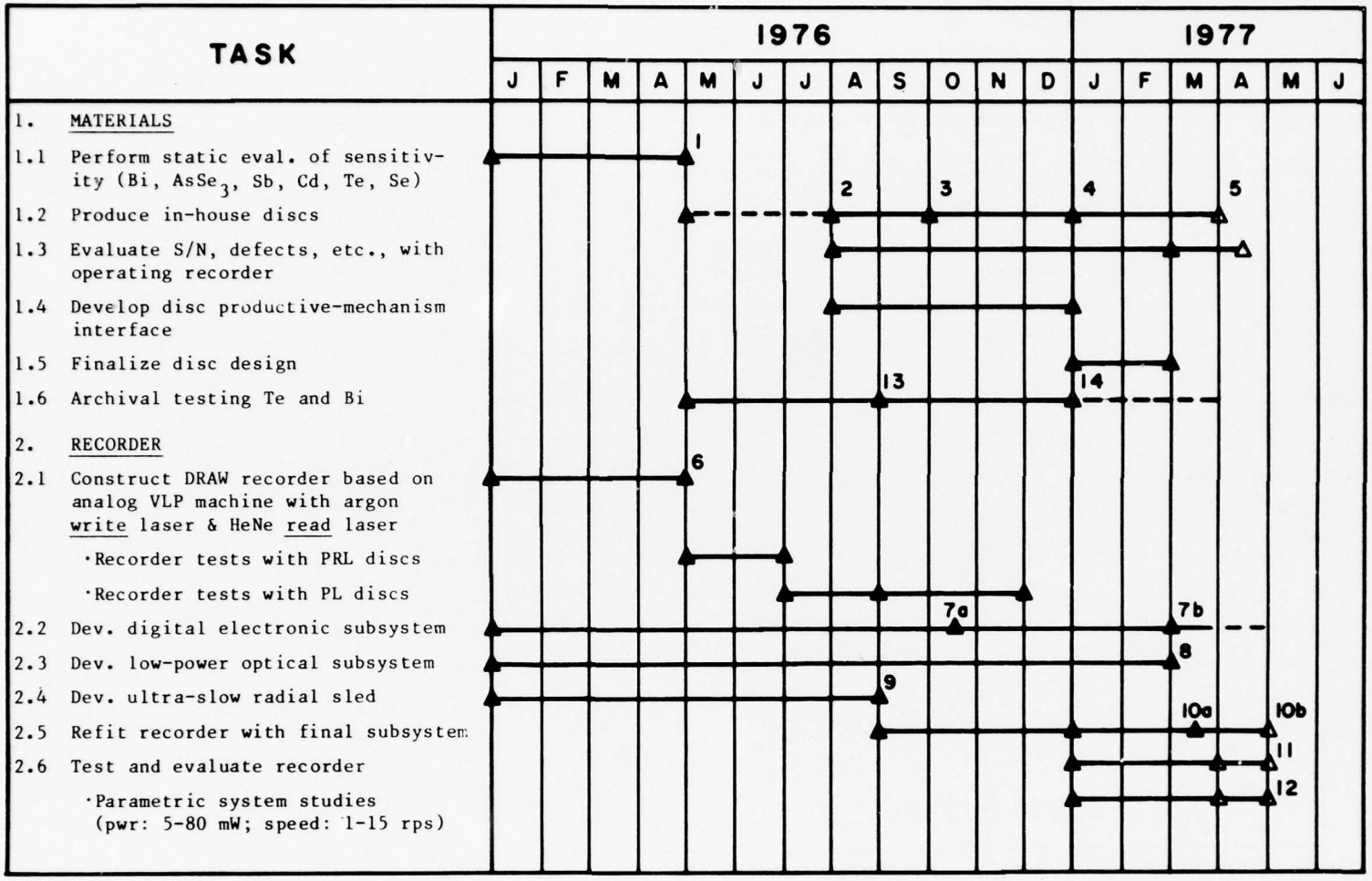

▲ *Completed tasks.*

Figure 1: Program Schedule for Development of Optical Disc Recorder

(Sht. 1 of 2)

TASK	1976 J	F	M	A	M	J	J	A	S	O	N	D	1977 J	F	M	A	M	J

PROGRAM MILESTONES

Milestone No.	Description
1	First narrowing of material choices complete.
2	Large-area deposition capability available.
3	Second narrowing of material choices complete.
4	Optimum material selected.
5	Deliverable discs available.
6	Recorder available for test.
7a	Characterization of recorder channel complete.
7b	Assy. of digital electronics subsystem complete.
8	Assy. of optical subsystem complete.
9	Assy. of improved radial sled complete.
10a	Final system assembly.
10b	System checkout complete.
11	Deliver laboratory prototype system.
12	Parametric system studies completed.
13	First lifetests on tellurium available.
14	First archival results tellurium and bismuth.

Figure 1: Program Schedule for Development of Optical Disc Recorder

(Sht. 2 of 2)

4. DISCUSSION

A new semi-clean room for fabricating tellurium discs is now operational. The room has all the facilities necessary to fabricate air sandwiches - including disc cleaning, vacuum deposition, and air sandwich bonding. Twenty air sandwiches were assembled so far, five of which are now undergoing channel-characterization testing at Philips Research Laboratories in the Netherlands. Preliminary indications suggest acceptable channel characteristics similar to that for bismuth.

With the implementation of an improved focus system, debugging of the prototype recorder is now completed. System investigations with the prototype recorder are planned for the next quarter.

The PRL recorder is now routinely used for materials evaluation. Single frequency test recordings have been made in several tellurium air sandwiches. The discs were played back in a special player called an "Integrator Player" with signal-to-noise better than 40 dB (see Fig. 2); this is more than adequate for digital recording. Digital information was also recorded in an air sandwich (Fig. 3). The fidelity of the digital recordings will be examined next quarter.

4.1 Archival Testing

Archival testing of various film materials and substrate combinations continues. No significant deterioration in sensitivity or optical properties has been observed for tellurium films on Glasflex PMMA substrate, the chosen disc system, at any of the four aging temperatures. Figure 4 plots the static sensitivity for one micron diameter holes at 750 ns exposure duration as a function of aging time. The recording spot had a power of about 3.8 mW and an Airy disc radius of 1 μm.

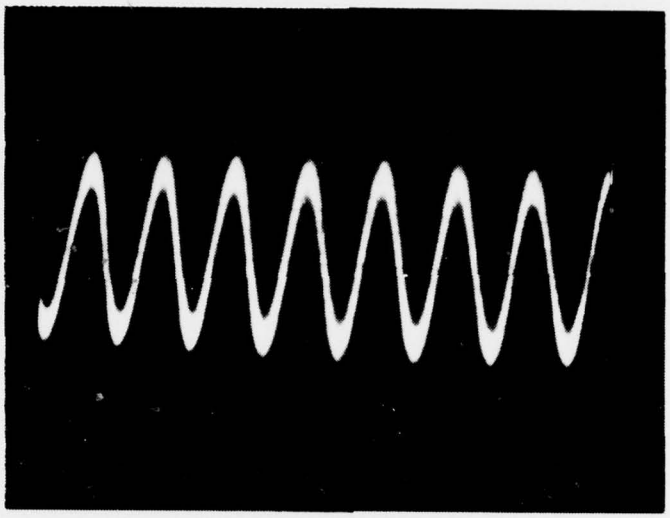

Figure 2: Playback of signal with 40 dB SNR.

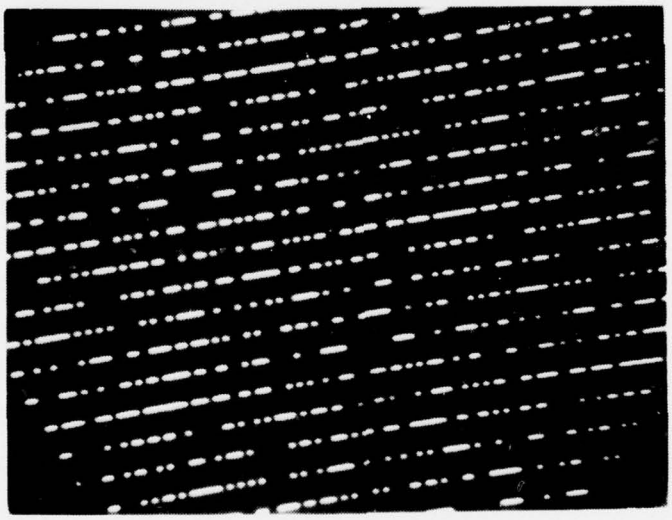

Figure 3: Data recorded in tellurium air sandwich disc.

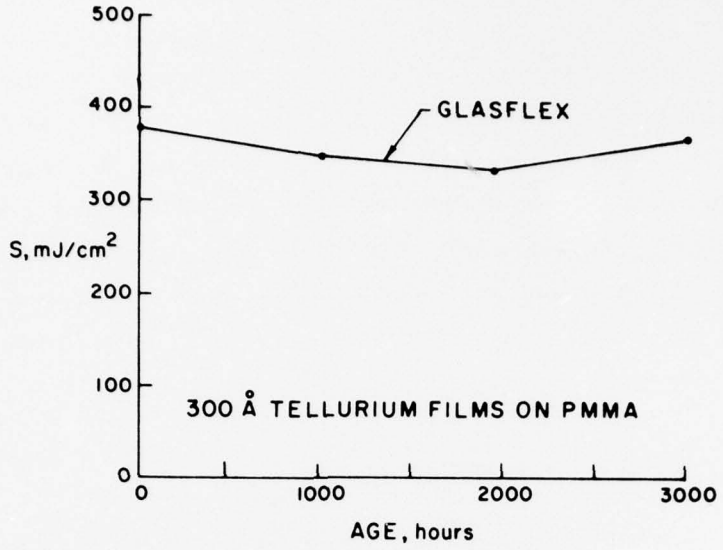

Figure 4: Best fit sensitivity at one micron as a function of ageing time.

No degradation has been observed after 3,000 hours at 90°C. Assuming that the degradation is an oxidation process with an activation energy of about 0.5 eV, this would correspond to a shelf life of 10 years. Humidity stress aging of tellurium samples and air sandwiches will begin next quarter.

4.2 Air Sandwich Discs

The disc dimensions have now been set. During the quarter the spindle hole diameter was standardized at $35^{+.0}_{-.1}$ mm - the same as that of a consumer videodisc. With minor modifications to the magnetic clamp, future air sandwich discs will be compatible with the spindle on the Magnavox videodisc player So as to further assure compatibility with the player, the static balance specification on future air sandwiches will be equivalent to that of a videodisc (<4-1/4 gm-cm). The cavity thickness has been tentatively set at 0.5 mm. The inner and outer radii of the air cavity are 6.5 cm and 14.5 cm, respectively.

The inner radius was chosen as large as possible, and the outer radius as small as possible, to provide maximum flexural stiffness. The diameter of the disc adaptor on the turntable will be enlarged from 7.5 cm to 9 cm to provide greater support for the disc. Calculations have shown that the average static droop of an air sandwich would be reduced from 0.23 mm, which has been measured recently, to 0.17 mm if this change is made. Nine (9) cm is the largest diameter which would still allow writing at an inner radius of 6.5 cm with the focus motor now in use.

4.3 Air Sandwich Fabrication

A new disc assembler was designed and built during the quarter (see Fig. 5). It is capable of mechanically implementing all

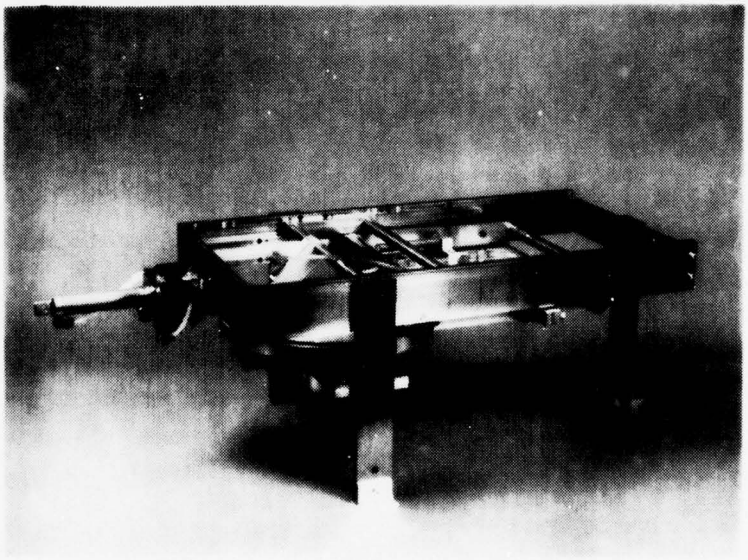

Figure 5: Air sandwich DRAW disc assembler.

of the adhesive assembly techniques that we have developed to date. In addition, it is capable of evaluating several new techniques not yet tried. Basically, it consists of two vacuum

hold-down plates which can be guided together in a parallel fashion by means of a four-bar linkage. Once in contact, the plates can be pneumatically subjected to a predetermined load. The maximum clamping force attainable is about 6600 newtons. The plates serve to hold the substrates and standoffs flat as the disc is laminated together. The lower vacuum plate - and an auxiliary plate - also serves to align the substrates and standoffs concentrically. The adhesive is dispensed from a pneumatically controlled hypodermic syringe. An upper guide serves to bring the dispenser into position as well as hold it in a standby location off to the side of the vacuum plates. The syringe itself is indexed into position over the outer and inner standoff zones. As the lower vacuum plate is rotated, by means of an electric motor, the adhesive is automatically dispensed during one complete revolution.

4.4 Disc Substrates

At the present time, air sandwich substrates are made from rectangularly shaped cast PMMA sheets. The sheets are scratched and shaped into roughly a circular disc. They are then machined to the final circular dimensions. No finishing is done on the thickness dimension. Efforts are being made to simplify the fabrication of cast sheet substrates as well as to completely circumvent the limitations of such substrates.

The Boston Die Cutting Co. has die cut 1 mm thick PMMA and 1/2 mm thick PVC sample discs for PL. Unfortunately neither material die cuts very sharply - the edges are very ragged and splintered. Even though it may not be satisfactory to die cut the final dimensions of the substrates and standoffs, die cutting to rough dimensions could save a considerable amount of work. A quote for substrate and standoff dies has been requested.

An alternative to cast sheet is to injection-mold the substrates. Injection molding offers the possibility of molding the standoffs directly into place and improving upon the thickness uniformity. As a result, it is possible that a concentrically located spindle-hole may provide adequate disc balance. At the present time, none of the injection molders spoken to are interested in making discs under the terms that we may be interested in.

The quality control agreement* reached with Glasflex Corp. is working satisfactorily.

A new shipment of Electroglas 500 CT sheet was found to be within the thickness tolerance.

1 mm thick Rohm PMMA cast sheet - available through the cooperation of PRL - has now been used to make recordable air sandwiches. Although the material being used (Rohm 218) is the least plasticized PMMA available, preliminary observations indicate that it is less dimensionally stable than the Glasflex Electroglas. Another potential drawback of the present allotment may be that it is masked with a wafer soluble layer. The layer is intended to mask the PMMA surface from scratches before disc processing. There is some concern, however, that not all the masking is removed during cleaning and that some residuals may remain on the substrate. Until the question is resolved, surface protection by lens tissue is preferred. The availability of unmasked sheet has not been determined.

4.5 Recorder Subsystems

A turntable was built from commercially available components (Fig. 6). It consists of a Kollmorgen Corp. pancake armature motor (Type U9M4) with the ball bearings removed and replaced by a Professional Instruments' rotary air bearing (Model 4B). The air bearing is directly coupled to one end of

* *For details see Appendix B of October-December 1976, ARPA Quarterly Technical Report.*

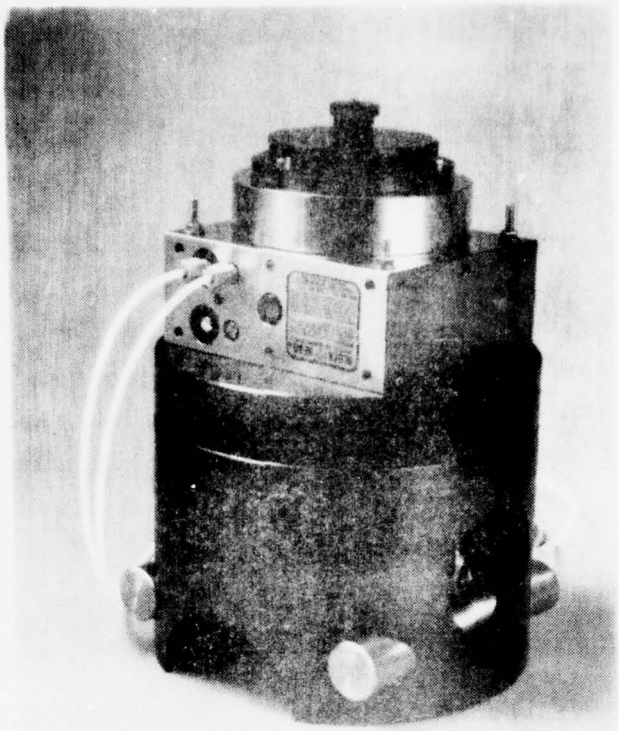

Figure 6: Kollmorgen turntable.

the motor shaft. A 2000-line optical encoder dial and single pick-off were mounted on the other end of the motor. Tests on the unit have shown it to be completely acceptable for slow speed digital recording applications.

The air bearing sled system was extensively tested at the component level and found to operate reliably at constant velocities as low as 1 μm/s. These results indicate that such a sled will meet the stability requirements to demonstrate slow-speed digital recording. The sled consists of a Dover #400-B (special) air bearing of rectangular cross-section, a linear electric motor, and a linear velocity transducer from Collins Corp. (#LMV-719 S22). A complete analysis and report of the results are given in Appendix A.

The recorder layout was finished and assembly is now underway. The machine will incorporate the backup sled and turntable. The focus motor is similar to that used on the PRL recorder. The optical system is similar to that of the prototype recorder. A 25 mW HeNe laser will be used for recording.

The lead screw sled was assembled as planned. The slow motion performance was tested by an interferometer, proximity detector, and by writing a continuous track on a disc. The tests show that the lead screw sled is adequate for the simple task of recording a uniform track with a pitch variation less than 10%. Although the sled does not offer rapid access, it is an interesting candidate for a two-sled recorder as described in the last quarterly report. Appendix B gives the test results on the lead screw sled.

4.6 Digital Electronic Subsystem

The tasks of data modulation and error encoding/decoding are proceeding well. The Miller modulator and demodulator were designed, debugged and rendered operational. The Miller Code was chosen to match the user's input data power spectrum to the channel response of the optical disc. The Miller modem was tested, working at data rates up to 2.5 Mbits/s.

The Linkabit digital encoder/ decoder was delivered. The Linkabit system together with the Miller modulator/demodulator form a simple digital subsystem necessary to record and playback digital data from an air sandwich disc. These tests are planned for the next quarter. A second backup convolutional encoder/decoder is being fabricated.

5. PLANS

1. Complete first characterization of Te films.
2. Analyze playback of digital information from air sandwich disc.
3. Continue dynamic testing and characterization of tellurium.
4. Begin humidity life test of tellurium films and air sandwiches.
5. Begin systems studies with PL recorder.
6. Continue work on encoder/decoders.

APPENDIX A

Precision Sled for DRAW Recording

by

R. McFarlane and M. Giebler

PRECISION SLED FOR DRAW RECORDING

by

R. McFarlane and M. Giebler

1. INTRODUCTION

This note describes the design and initial performance measurements of a closed loop essentially frictionless sled for translating the recording and playback optics of a DRAW recorder, to produce a spiral information track on the disc.

Previous sleds, especially those used for video disc mastering, relied on precise lead screw, hydraulic or friction drives operated open loop or without velocity error correction. Such systems were expensive and usually quite large to provide stability during the recording interval and required a heavy maintenance schedule.

The sled described herein (see Fig. 1) uses a linear electric motor with air bearing coupling. The instantaneous velocity is sensed by an inductive velocity transducer which produces a proportional voltage for servoing the motor to a constant velocity. This configuration of sled provides compactness and the potential for improved uniformity of velocity during the recording cycle. The first step in implementing a closed loop system is to determine the transfer function of the linear motor. This is followed by examining the transfer function of the motor transducer combination to determine whether compensation for stability is required.

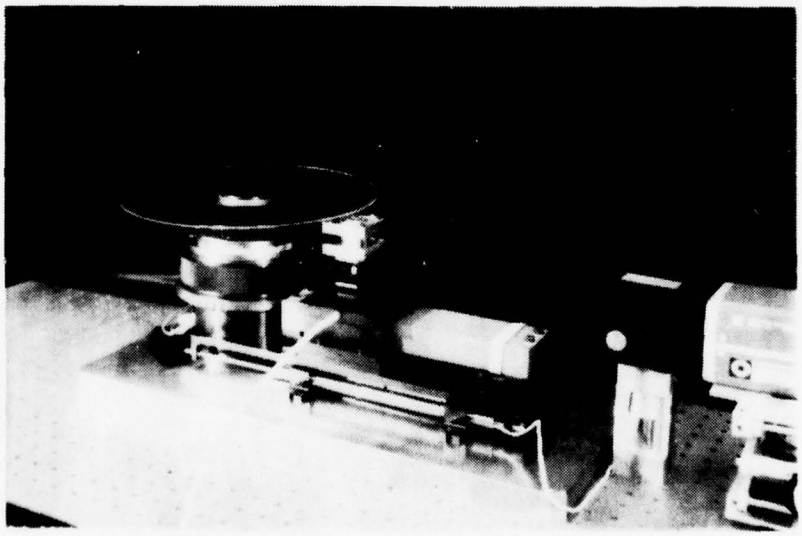

Figure 1: Recording system showing sled.

2. MOTOR TRANSFER FUNCTION

The electric motor transfer function is obtained by combining the electrical terminal behavior at the input with the output force equation.

The force equation of the linear motor is

$$F_g = \frac{Md^2x}{dx^2} + \frac{Ddx}{dt} + Cx + F_F + F_L$$

F_g = generated force
M = mass moved
D = coefficient viscous friction
C = spring constant
F_F = friction force
F_L = load force

The electrical equivalent circuit of the motor is shown

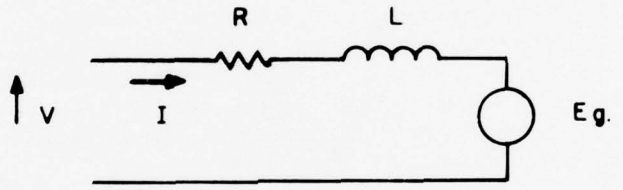

and

$$V = \frac{LdI}{dt} + RI + E_g$$

where E_g is the generated back emf and

$$E_g = K_E v$$

K_E = emf constant
v = velocity

Therefore

$$V = \frac{LdI}{dt} + RI + K_E v$$

For constant magnetic field

$$F_g = K_F I$$

K_F = force constant

Using Laplace transform and assuming

(a) $F_F = 0$ air bearing
(b) $F_L = 0$ no loading along direction of motion
(c) no initial conditions.

We obtain

$$V(s) = (sL + R)\ I(s) + K_E s x(s)$$

$$F_g(s) = K_F I(s)$$

$$F_g(s) = Ms^2 x(s) + Dsx(s) + Cx(s)$$

From which is obtained the transfer function

$$G_m(s) = \frac{x(s)}{V(s)} = \frac{K_F}{(sL+R)(s^2M+SD+C)+K_F K_E s}$$

$$G_m(s) = \frac{K_F}{LMs^3+(RM+LD)s^2 + (DR+CL+K_E K_F)s + RC}$$

Case I $D \approx 0$ low viscous damping
$C = 0$ no spring forces
$L \approx 0$ low inductance

When D = 0 and C = 0 the transfer function becomes

$$G_m(s) = \frac{K_F}{LMs^3 + RMs^2 + K_E K_F S}$$

$$G'(s) = \frac{v(s)}{V(s)} = \frac{K_F}{LMs^2 + RMs + K_E K_F}$$

The roots of the characteristic equation are

$$P_1, P_2 = \frac{-RM \pm \sqrt{(RM)^2 - 4LMK_EK_F}}{2LM}$$

For low inductance

$$L << \frac{R^2M}{K_EK_F}$$

the approximation $\sqrt{1-x} \cong 1 - x/2$ can be applied

$$\sqrt{(RM)^2 - 4LMK_EK_F} \cong RM \frac{(1-2LK_EK_F)}{R^2M}$$

and

$$P_1 \cong \frac{-K_EK_F}{RM} \qquad P_2 \cong \frac{-R}{L}$$

$$G'_m(s) = \frac{1/K_E}{(\tau_m S+1)(\tau_e S+1)}$$

$\tau_m = \frac{RM}{K_EK_F}$ mechanical time constant

$\tau_e = \frac{L}{R}$ electrical time constant

The following constants were measured:

(1) $R = 3.3$ ohms — motor excited

(2) $L = 0.6 \times 10^{-3}$ hy

(3) $M = 1.36$ kg — (Measured force and acceleration)

(4) $K_F = 1.08$ N/A* — (Measured as the stall force. See Figure 2).

---

* N/A = Newton/Ampere

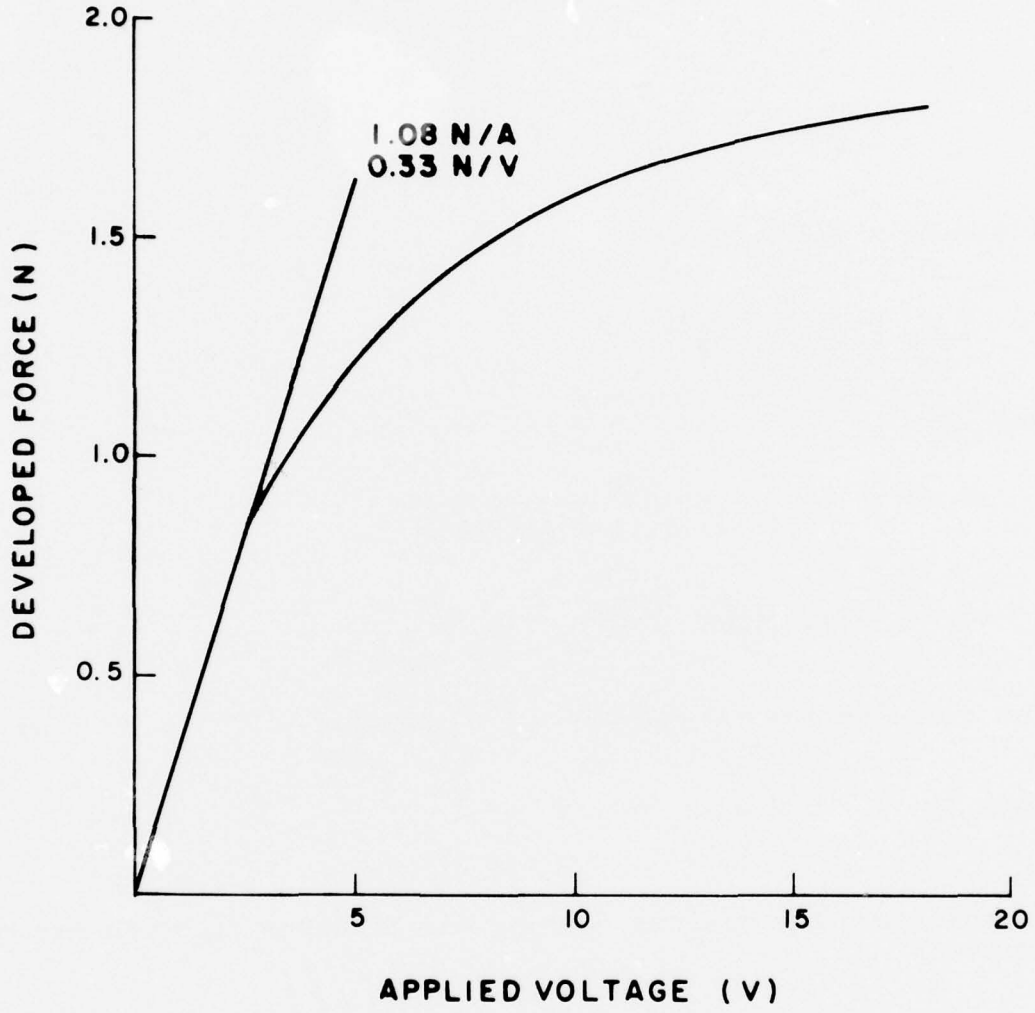

Figure 2: Developed force vs. voltage of sled linear motor.

In MKS units

$$K_F(N/A) = K_E(V/m\ sec^{-1})$$

so that

$$\tau_m = \frac{RM}{K_F^2} = \frac{3.3\ ohm \times 1.36\ kg}{(1.08\ N/A)^2}$$

$$\cong 3.8\ sec$$

$$\tau_e = \frac{L}{R} = \frac{6 \times 10^{-4} hy}{3.3\ ohm} \cong 1.8 \times 10^{-4}\ sec$$

Since $K_E = 1.08\ V/m\ sec^{-1}$

$$1/K_E = 0.926\ \frac{m/sec}{V}$$

and

$$G_m'(s) = \frac{0.926}{(3.8\ s+1)(1.8 \times 10^{-4}s+1)}$$

$$= \frac{0.926}{(3.8)s+1}\ \frac{m/sec}{V}$$

for frequencies of interest (0 - 1 kHz).

Case II $C = 0$

$L \cong 0$

If the motor has viscous damping the transfer function may be written

$$G_m'(s) = \frac{K_F}{LMs^2 + (RM+LD)s + (DR+K_EK_F)}$$

Since $L \cong 0$

$$G_m'(s) = \frac{K_F}{LMs^2 + RMs + (DR+K_EK_F)}$$

and

$$\tau_m = \frac{RM}{DR + K_EK_F}$$

if

$$L << \frac{R^2M}{DR + K_EK_F}$$

Therefore the effect of small amounts of viscous damping on the motor transfer function is to decrease the mechanical time constant.

Case III D = 0

$$G_m(s) = \frac{K_F}{LMs^3 + RMs^2 + (CL+K_EK_F)s + RC}$$

If the spring constant C is of a magnitude such that $CL << K_EK_F$, or $C < 10^3$ N/M, the characteristic equation becomes

$$LMs^3 + RMs^2 + K_EK_Fs + RC = 0$$

and substituting the values of known constants

$$(8.3 \times 10^{-4})s^3 + (4.48)s^2 + (1.17)s + 3.3C = 0$$

For all values of C, one root of the equation remains essentially constant. This root, $-1/\tau_e \cong 5397$ is the reciprocal of the electrical time constant. The other two roots P_2 and P_3 are real and negative for small values of C and become complex conjugates in the left half of the s-plane as C is increased. For these values the motor's response to a voltage step input would exhibit damped oscillation.

The locus of these two roots in the s-plane as a function of C is shown in Figure 3. The roots become imaginary when $C = 1.9 \times 10^3$ N/m (173.6 oz/in). The undamped osicillation which would result is at a frequency

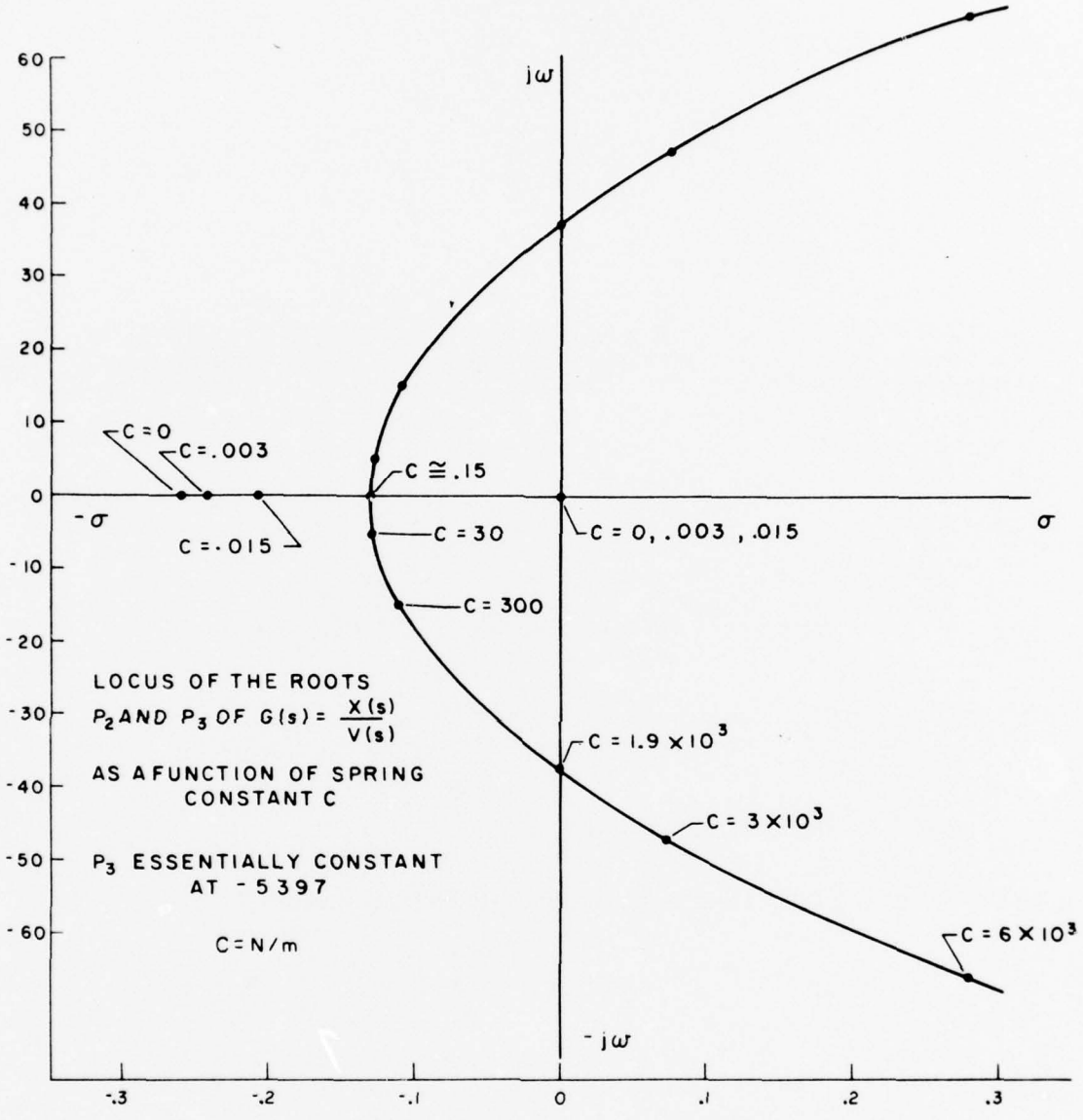

Figure 3: Complex roots of motor characteristic equation.

$$f = \frac{\sqrt{3.3C}}{4.48} = 37.4 \text{ Hz}$$

For the expected value of C of 1.5 N/m due to air hose and electrical cables, the imaginary part of the roots is not significant.

The above discussion indicates that, for the purpose of designing the sled servo, the approximate transfer function of Case I is sufficiently accurate. Subsequent sections will therefore assume that motor transfer function to be

$$G_m(s) = \frac{x(s)}{V(s)} = \frac{0.926}{s(3.8s + 1)} \frac{m}{V}$$

$$G'_m(s) = \frac{v(s)}{V(s)} = \frac{0.926}{(3.8s + 1)} \frac{m/sec}{V}$$

3. SERVO DESIGN

The frequency response of the linear motor was measured by exciting the armature with variable frequency voltage and measuring the displacement of the sled with a linear proximity detector. The displacement as a function of frequency shown in Figure 4 decreased at a rate of 40 dB per decade as predicted in the previous section.

For closed loop operation, the transducer to provide the feedback signal was a linear velocity sensor shown in Figure 5. The motion of the magnet induces a voltage in the coil proportional to velocity. The transducer's response is 9.8 V/m/sec. To minimize inductive cross talk between the excited linear motor coil and the transducer, the transducer coil was mounted on the moving collar of the air bearing

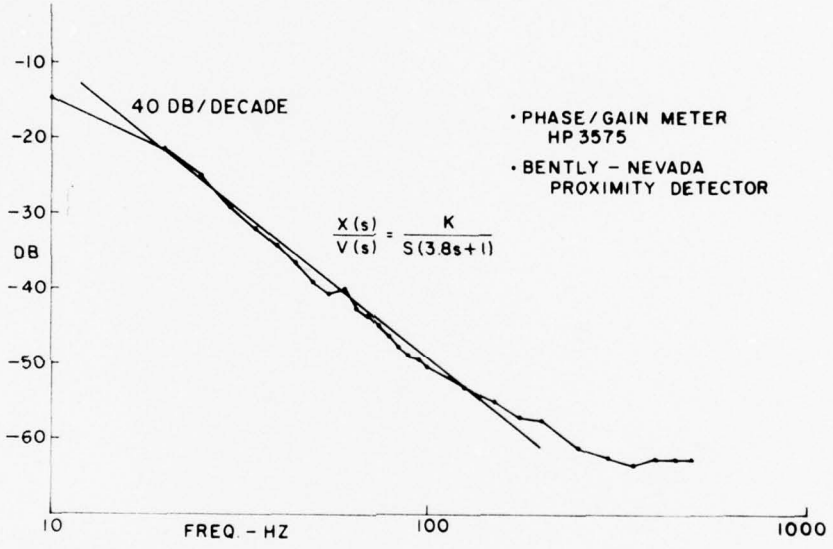

Figure 4: Frequency response of sled linear motor.

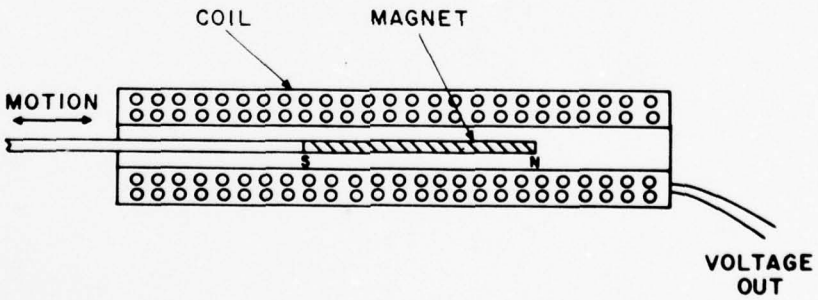

Figure 5: Linear velocity sensor.

so that the ends were equidistant from the motor coil. The magnet rod was stationary. The gain and phase responses of the motor transducer combination are shown in Figures 6 and 7. The behavior of the gain-frequency response is predictable to about 100 Hz. At frequencies between 100 Hz and 3 kHz several mechanical resonances occurred.

Some of the resonances were traced to vibration of the magnet rod induced by motion of the transducer coil because some contact between the two could not be avoided. The computed resonant frequencies of the rod with both ends fixed were 380 Hz and 1070 Hz.

A proximity detector was used to measure the displacement of the magnet rod as a function of frequency with constant voltage level at the motor input. Figure 8 shows the spectrum of displacement with significant resonances at 52 Hz, 400 Hz, and 890 Hz. Since the resonance at 52 Hz did not affect the frequency response of the motor transducer combination, a lag network at 120 Hz was used to roll off the response where significant mechanical resonances occurred.

The general trend of the gain-frequency response above 200 Hz is that of increasing gain as a function of frequency. This is due to the electrical self resonance of the transducer coil centered at approximately 15 kHz. The response at that frequency is equal to the response in the 70-80 Hz range so that the electrical resonance of the transducer coil cannot be ignored.

To reduce the effect of the electrical resonance of the transducer, the feedback circuit was band-limited by an integrator to about 500 Hz.

Closed loop behavior with the above compensation was stable but the system was not particularly effective in correcting low frequency velocity errors due to cable drag. A large low frequency gain is needed because of the low sensitivity of the motor and transducer. The transducer delivers approximately 10 μ V per μm/sec. At a nominal speed of 6 μm/sec (for 2μm track pitch at 3 rps disc speed) a 10% variation in speed results in a 6 μ V tachometer signal. The drag produced by the flexible air hose was found to be 0.14 N. Since the linear motor sensitivity is approximately .33 N/V a 0.41 V correction signal is required for this error so that loop gain must be of the order of 100 dB. To improve the low frequency response, a lag at zero frequency was added to provide essentially infinite dc gain. To retain stability a lead at .12 Hz was added. A block diagram of the servo is shown in Figure 9 and the schematic of the electrical section in Figure 10. The open loop frequency response is shown in Figure 11. Measurements of the frequency response were done without the low frequency enhancement to avoid the effects of saturation.

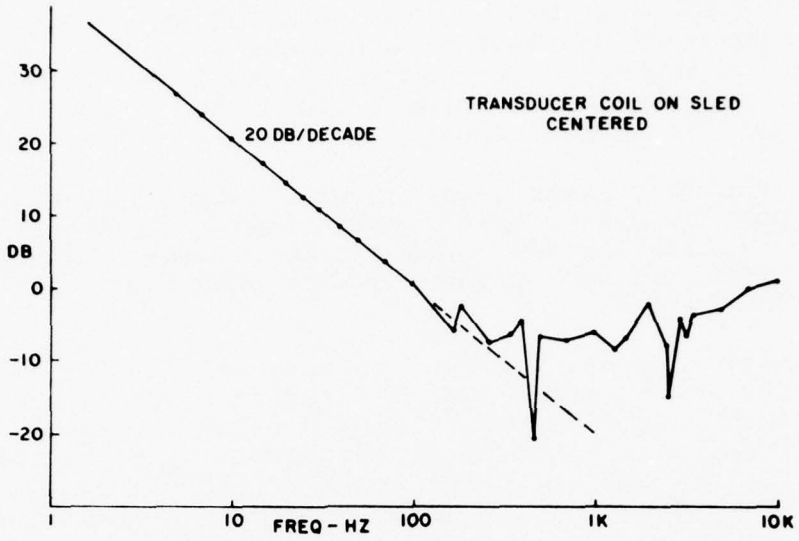

Figure 6: Gain vs. frequency of sled-transducer.

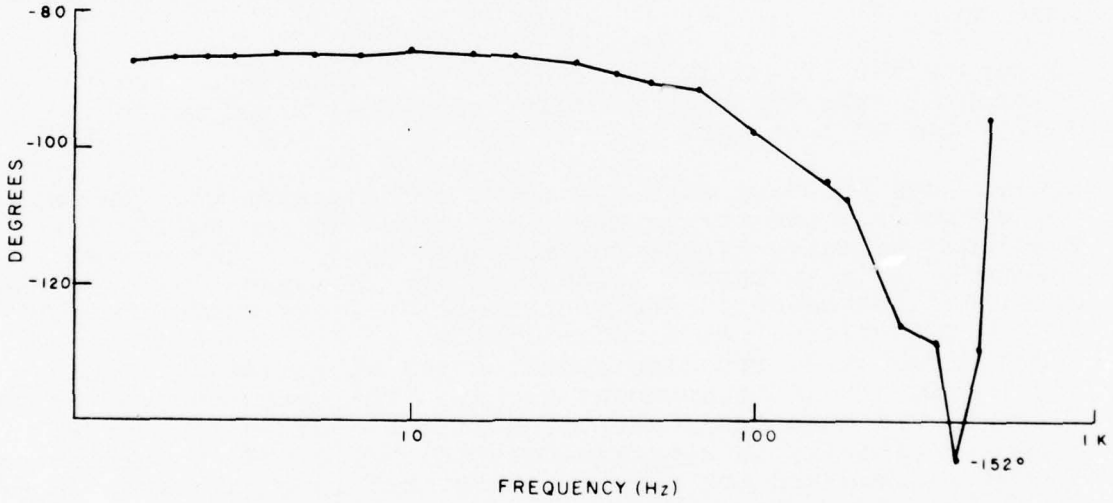

Figure 7: Phase vs. frequency of sled-transducer.

Horiz - 100 Hz/Div.
Resonances at 52 Hz, 400 Hz and 890 Hz.

(a)

(b)

Note: There are two exposure, one with (a), and one without (b) excitation.

Figure 8: Vibration spectrum of transducer magnet rod.

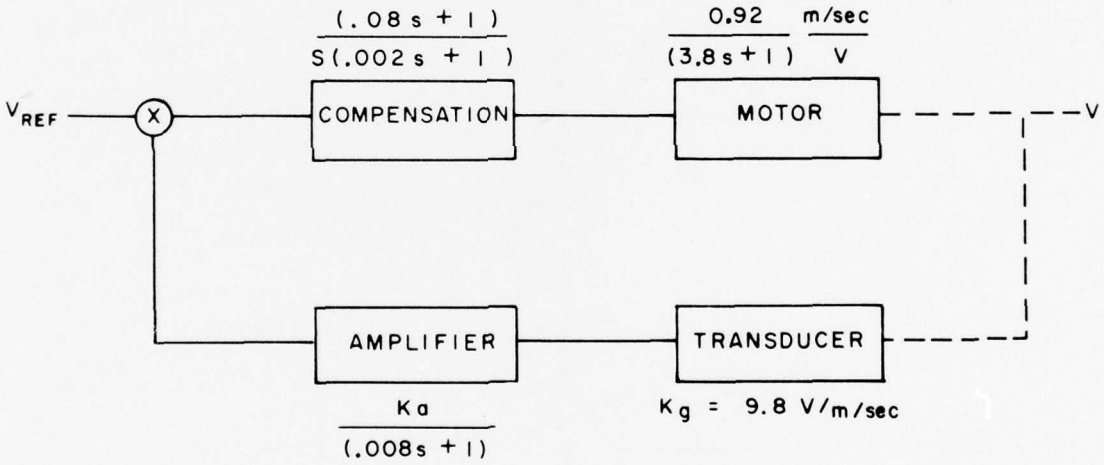

Figure 9: Block diagram of sled servo.

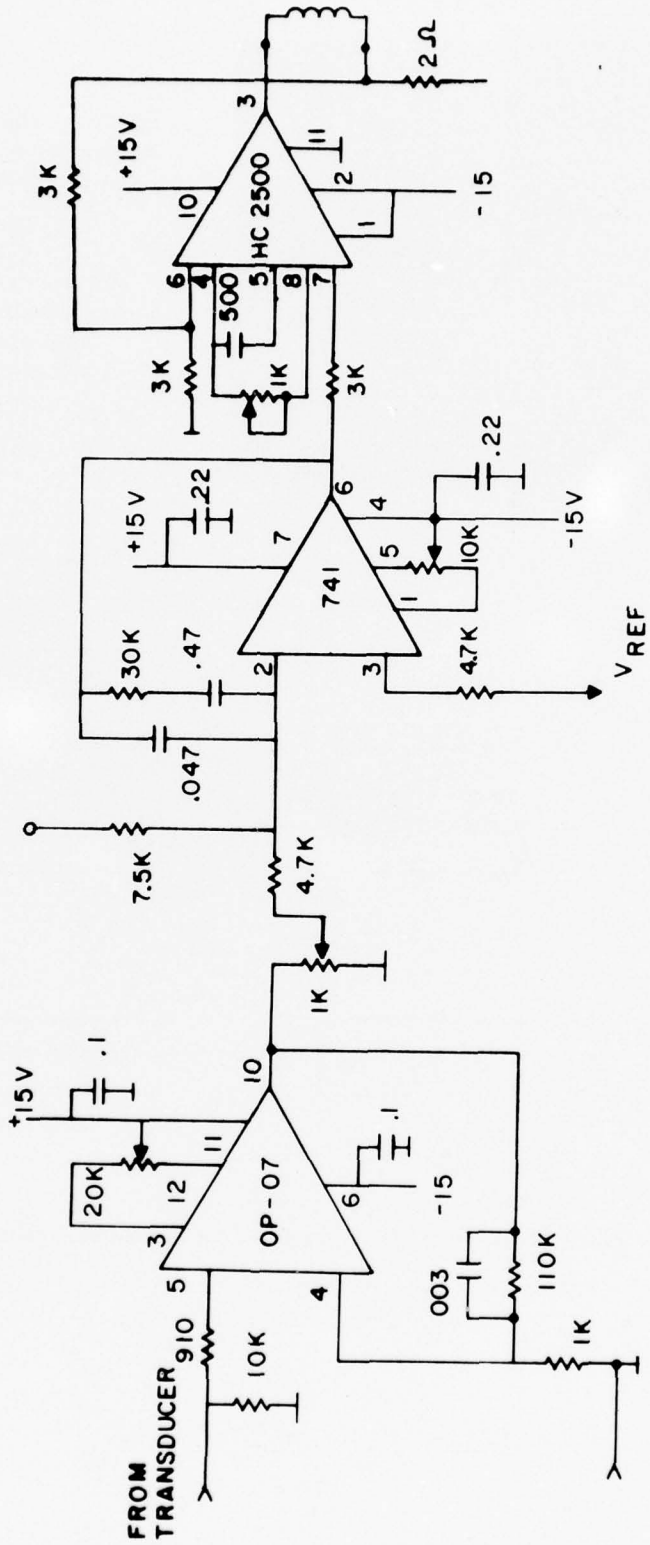

Figure 10: Sled servo electronics.

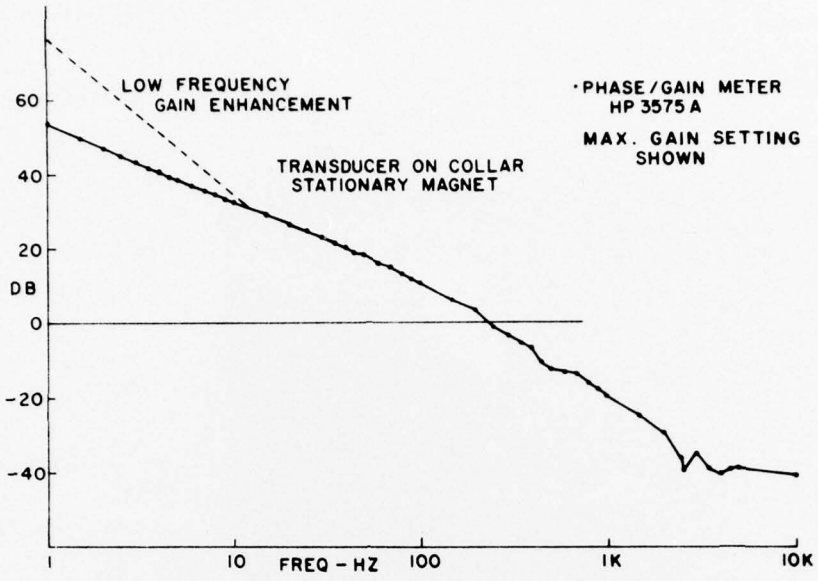

Figure 11: Open loop gain vs. frequency of sled servo.

4. SYSTEM BANDWIDTH

The bandwidth of the system was determined by examination of the step response and by a point by point measurement of gain and phase as a function of frequency.

The step response of the unloaded sled is shown in Figure 12.

Figure 12: Closed-loop step response of sled. 30 µm/s step input. Rise time ≈ 2 ms (sled unloaded).

The magnitude of the step in velocity is approximately 30 µm/s. An estimate of the rise time of the response is 2 ms yielding a bandwidth of 175 Hz. This value agreed with the bandwidth determined from the frequency response of Figures 13 and 14. However, these figures show that the useful bandwidth, when the optical system is assembled on the sled, will be closer to 100 Hz.

The difference between the velocity step input and the closed loop response gives a measure of the system's ability to correct for an input impulse of force.

Figure 15 shows that an input impulse of force produces a velocity step input. The transient velocity error is a damped sinusoid resulting in a constant displacement error.

The velocity error is:

$$v_e = v_m e^{-at} \cos \omega t$$

$$= \frac{I}{m} e^{-at} \cos \omega t$$

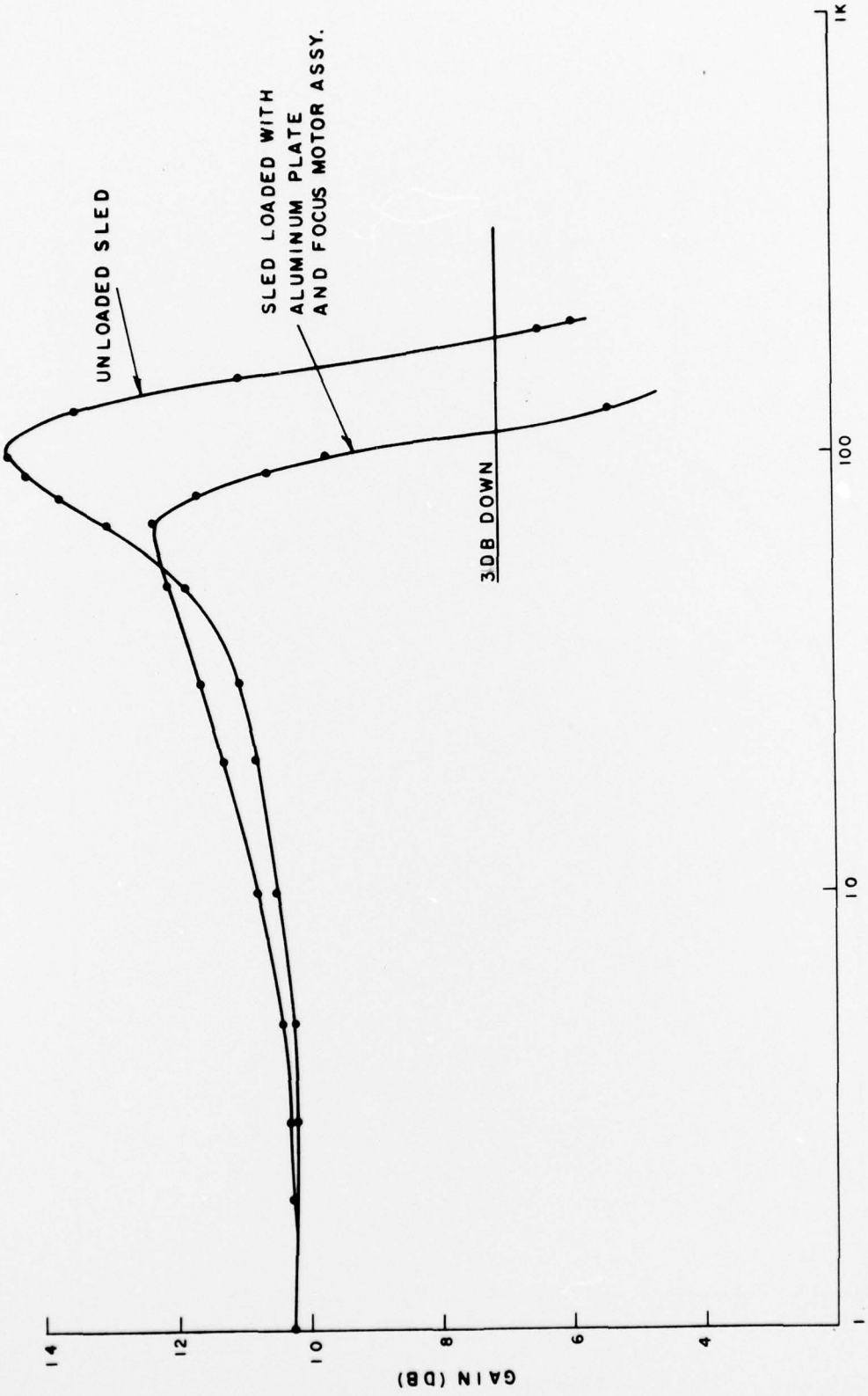

Figure 13: Closed loop gain vs. frequency of sled.

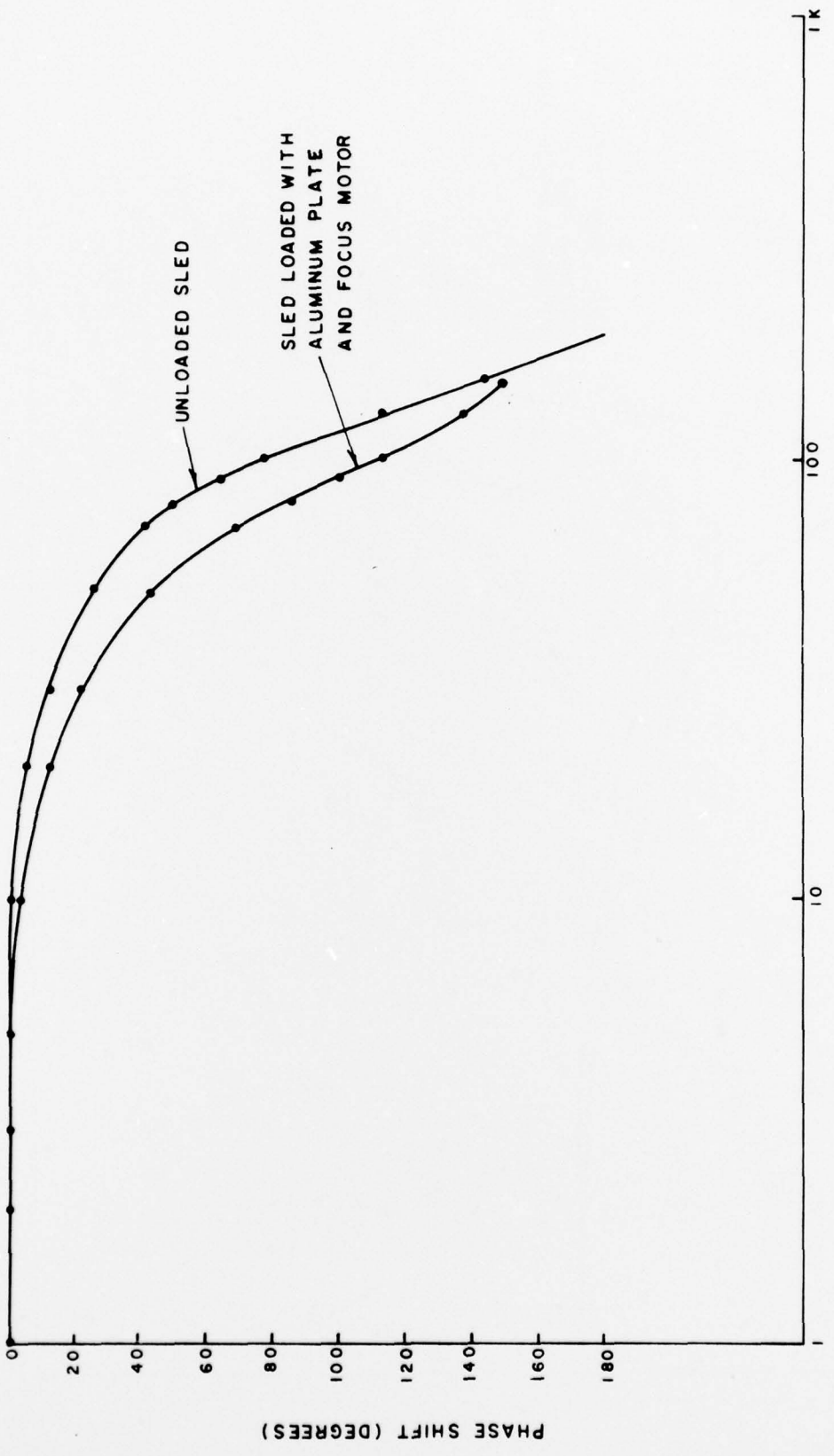

Figure 14: Closed loop phase vs. frequency of sled.

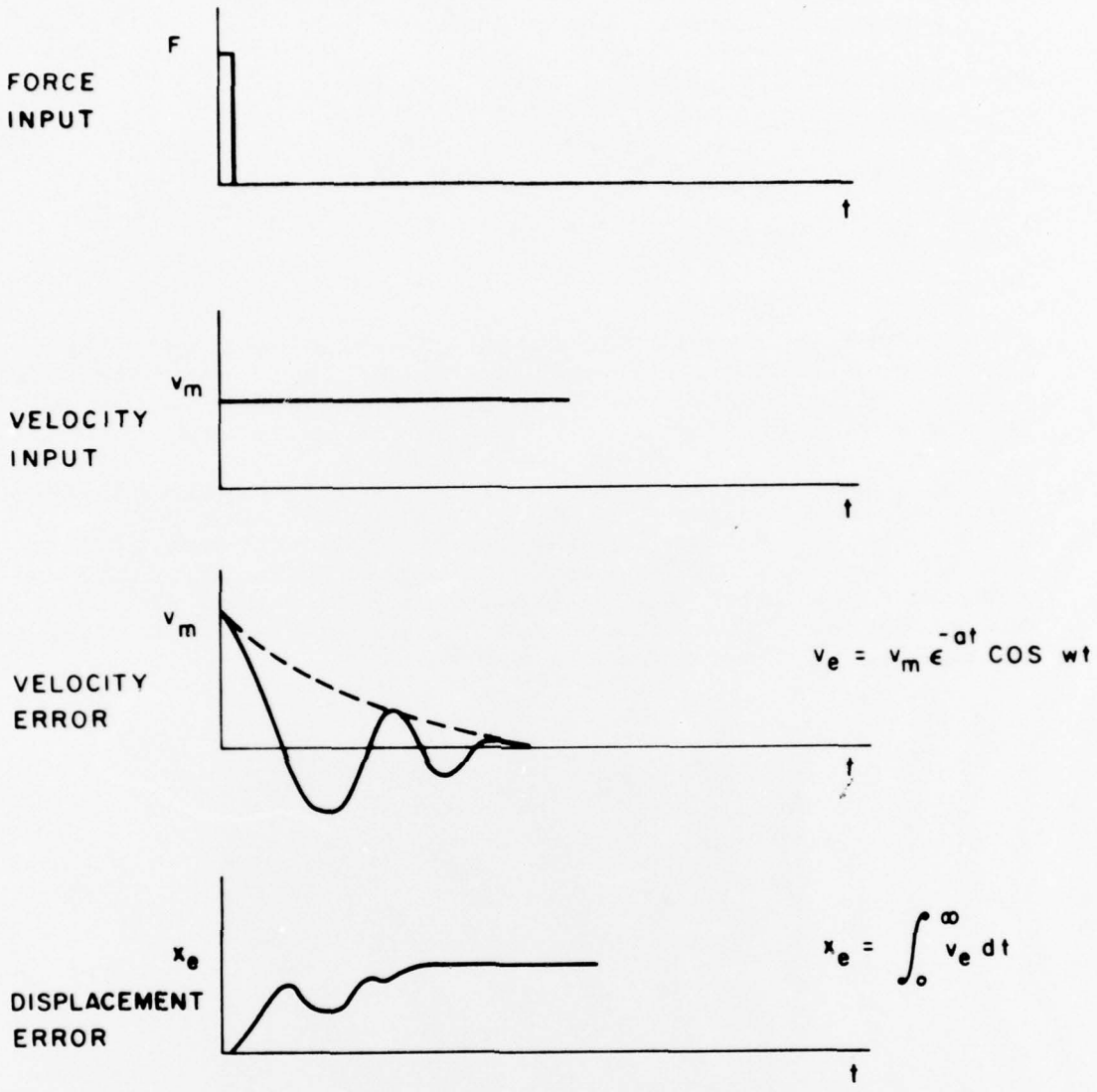

Figure 15: Transient velocity and displacement errors from an impulse force input.

where,

I = impulse of force or change in momentum
m = moving mass of the system.

The resultant displacement error is:

$$x_e = \frac{I}{m} \int_0^\infty \varepsilon^{-at} \cos wt \, dt$$

$$= \frac{I}{m} \left(\frac{a}{a^2 + w^2} \right).$$

From Figure 16, the actual transient velocity error, the frequency of the damped oscillation, w, is approximately 628 and the reciprocal of the damping time constant, a, is 140. The mass is 1.36 kg.

If the allowable displacement error is 0.2 μm, the maximum permissible input impulse force is 8×10^{-4} kg m/sec (Newton/sec). For an impulse covering an interval of 1 ms, the maximum force is 0.8 Newton (3 oz approximately). This is the maximum force which can be applied to the moving sled platform and is therefore much less than the allowable force which can be applied to the recorder's table.

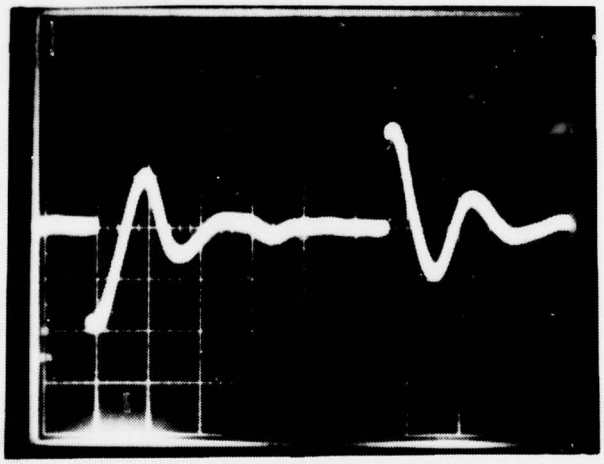

Figure 16: Velocity error to a step input. (10 ms/div.).

5. SLED PERFORMANCE

The uniformity of the sled velocity was measured over limited ranges by means of a linear proximity detector. The output of the detector was displayed on a oscilloscope with slow sweep rate. Figure 17 shows three traces of the sled moving at a nominal velocity of 57 μm/s, one at the center of the required 8 cm sled range and one at each extreme. These traces show the sled velocity to be linear to within 10% over the range. The short term error from track-to-track is too small to measure. Figure 18 shows the velocity variation as a function of sled position over the maximum range of 9 cm. The large velocity variation during the last centimeter of travel was traced to sensitivity variation of the velocity transducer as a function of magnet-to-coil position. This sled operates at constant velocities as low as 1 μm/sec. Figure 19 shows the linearity of the velocity at approximately 2.9 μm/sec.

It should be noted that for the above measurements, the sled was operated in a near ideal environment of an air supported table and without the normal system vibration inputs. The ultimate test of the linearity of the sleds velocity will be in the production of a recording under specified environmental conditions.

6. CONCLUSIONS

The preliminary tests indicate that the sled may possess the necessary stability and linearity for incorporation in an optical DRAW recorder operating at disc speeds of 3 rps with a 2 μm track pitch.

Improvements of the sled in terms of uniformity of velocity can be achieved by use of a velocity transducer having more linearity with respect to sled position.

The bandwidth requirement for the sled will finally be determined by the expected force inputs from the final recorder environment. In the interim, an investigation has begun to determine the maximum system and environmental force inputs which can be applied to the sled in the present configuration while maintaining a 10% maximum variation of velocity.

ACKNOWLEDGMENT

We express thanks to Victor Klebanoff for computations made in analyzing the characteristic equation of the linear motor.

Vertical (31.2 μm/div) - Horizontal (20 ms/div)

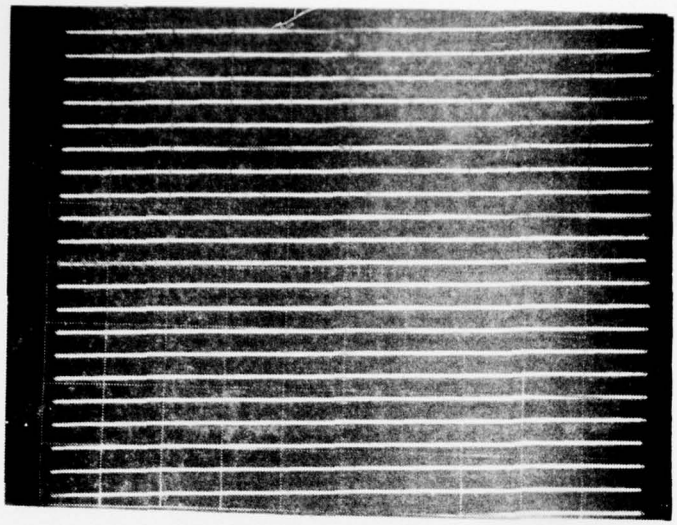

Sled zero position
57.5 μm/s

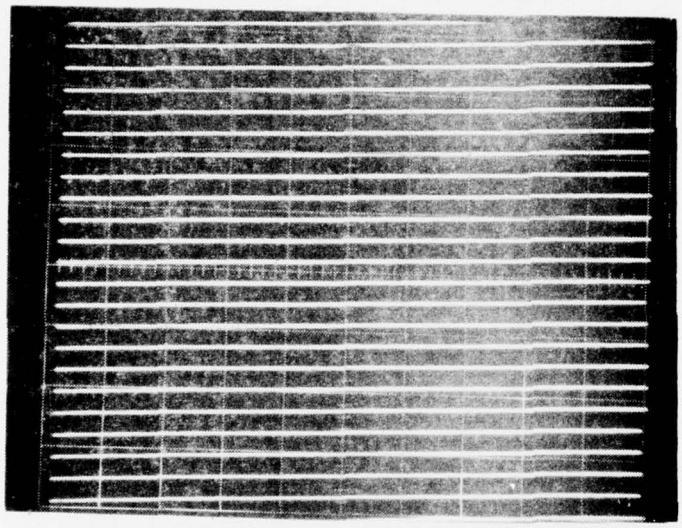

Sled at 4.5 cm
53.8 μm/s

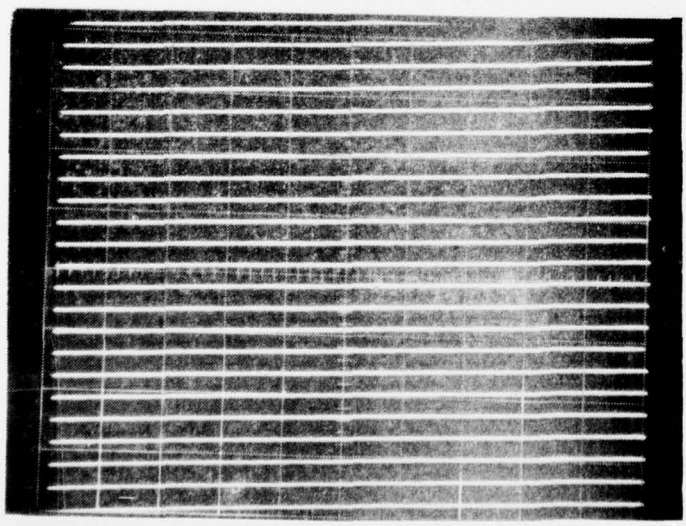

Sled at 8 cm
61.7 μm/s

Figure 17: Sled velocity measured at 3 points of an 8 cm excursion.

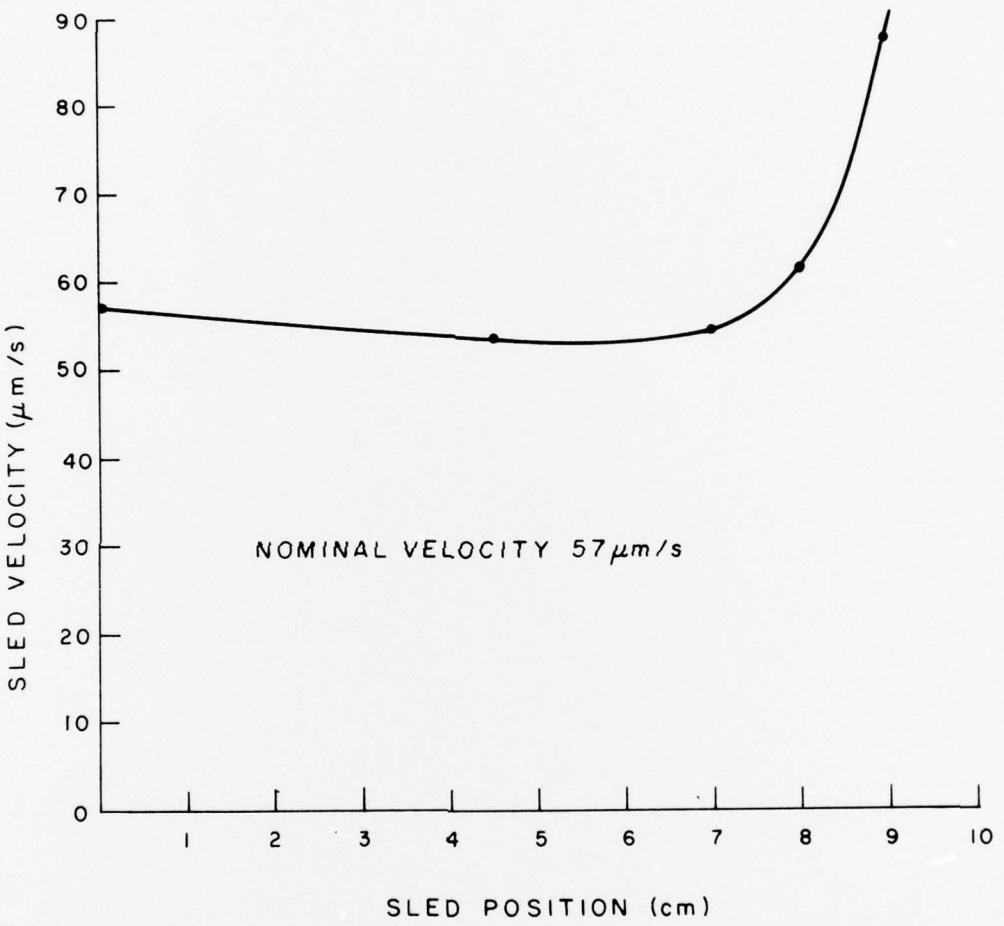

Figure 18: Variation of sled velocity with position.

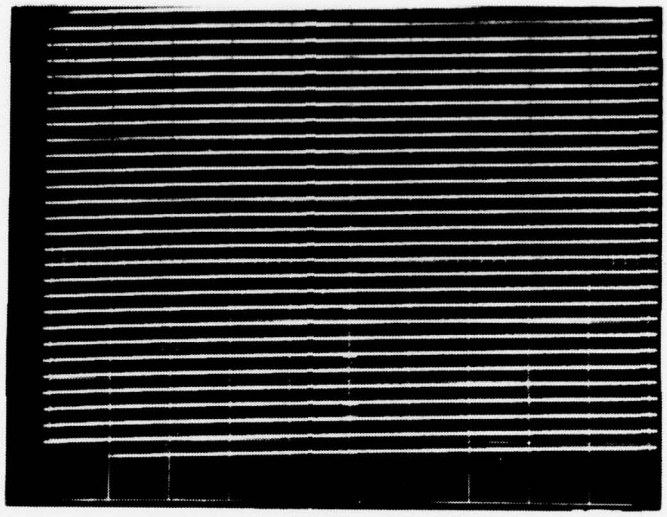

Figure 19: Oscilloscope trace of sled velocity over a limited range.

APPENDIX B

Test Results for Lead Screw Sled

by

F. Zernike

TEST RESULTS FOR LEAD SCREW SLED

by

F. Zernike

The lead screw sled was tested in three different ways: (a) by interferometer, (b) by proximity detector, and (c) by writing a continuous track on a disc. Tests (a) and (b) showed the motion of the sled to be uniform to within 10% over short (~1 mm) distances. Test (c) is, of course, the most sensitive and also the most meaningful test, since it uses one sled in its ultimate application. The test was run using a glass disc and static focussing. In this manner, a track could be written over approximately 250° of the disc's rotation. A track pitch of 2.5 μm was arbitrarily selected. The written tracks were examined: by microscope; by visual examination of the appearance of the entire disc; and by observing variations of the diffraction pattern as the disc is translated through a 2 mm diameter HeNe laser beam.

Photographs showing the appearance of the tracks under a microscope are shown in Figure 1. The figure is a composite showing tracks at 3 locations at intervals equal to one half turn of the lead screw. It can be seen that the track spacing variation

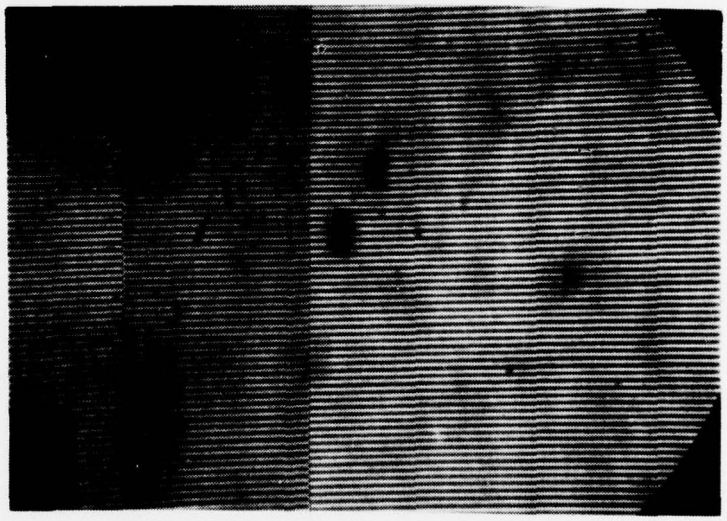

Figure 1

between R and R + 1/2 turn (of the lead screw) is larger than between R and R + 1 turn. A similar pattern is quite obvious by visual examination of the entire disc where bands of about 0.1" width appear (equal to the pitch of the lead screw). The diffraction pattern showed a similar result. As the disc is translated, the distance between the 0 order and the first order diffraction patterns varies about 2.5%.

In conclusion, it appears that this sled, even in its present form, is adequate. It should be noted, however, that in this first model the carriage slides directly on the lubricated ways. In addition, some run-out was present on the 360:1 worm and gear combination. In an improved model, Teflon carriage bearings could be used with a better gear reduction.